BNAM2012
Joint Baltic-Nordic Acoustics Meeting
June 18th - 20th 2012 Odense, Denmark

Numerical study of acoustic streaming and radiation forces on micro particles

Mads J. Herring Jensen[a], Peter Barkholt Muller[b], Rune Barnkob[c], and Henrik Bruus[b]

(a) COMSOL A/S, Diplomvej 373, 2800 Kgs. Lyngby, Denmark, mads@comsol.dk

(b) Department of Physics, Technical University of Denmark,
DTU Physics Building 309, DK-2800 Kongens Lyngby, Denmark, bruus@fysik.dtu.dk

(c) Department of Micro- and Nanotechnology, Technical University of Denmark,
DTU Nanotech Building 345 East, DK-2800 Kongens Lyngby, Denmark, rune.barnkob@nanotech.dtu.dk

We present a numerical study of the transient motion of micro particles in a microfluidic chip when influenced by acoustic forces. The system is driven in the MHz range and tuned to resonance. The forces on the particles are twofold: 1) acoustic radiation forces acting directly on the particles, and 2) Stokes drag from the induced acoustic streaming flow. Both effects are second order and require the solution of the full linearized Navier-Stokes equation in order to be captured correctly. The model shows the transition from streaming drag to radiation force dominated regimes. The transition is studied in terms of the particle size.

1 Introduction

Acoustofluidics and ultrasound handling of particle suspensions is a research field in rapid growth both concerning physical characterization and optimization of the devices as well as biological applications [1,2]. There has been a substantial advancement in understanding the fundamental physics of biochip acoustophoresis, which have been achieved through full-chip imaging of acoustic resonances [3], particle handling by surface acoustic waves [4–8], multi-resonance chips [9], advanced frequency control [10,11], on-chip integration with magnetic separators [12], acoustics-assisted microgrippers [13], acoustic programming [14], bandpass filters [15], and *in situ* force calibration [16,17].

Recently, Augustsson *et al.* have carried out detailed measurements of the acoustophoretic microparticle velocities in a microchannel by using a temperature-controlled and automated micro-PIV system [18]. These measurements, among others, create a need for improved numerical tools to simulate the motion of particles as they are influenced by acoustic forces. In this work we use the finite element software COMSOL Multiphysics 4.2a [20] to carry out a numerical study of the acoustophoretic motion of particles influenced by the acoustic radiation force due to scattering and the Stokes drag force of the acoustic streaming arising due to viscous effects at solid wall boundaries.

2 Perturbation theory

Briefly, and to establish our notation, the full acoustic problem in a fluid, which before the presence of any acoustic wave is quiescent with constant temperature T_0, density ρ_0, and pressure p_0, is described by the four scalar fields pressure p, temperature T, density ρ, and entropy s per mass unit as well as the single velocity vector field $\boldsymbol{v}$. The two thermodynamic relations

$$d\rho = \frac{\gamma}{c_0^2}\,dp - \alpha\rho\,dT, \quad \text{with} \quad \alpha = -\frac{1}{\rho_0}\left(\frac{\partial\rho}{\partial p}\right)_p, \tag{1a}$$

$$ds = \frac{c_p}{T}\,dT - \frac{\alpha}{\rho}\,dp, \tag{1b}$$

can be used to eliminate ρ and s, so that we only need to deal with the acoustic perturbations in temperature T, pressure p, and velocity $\boldsymbol{v}$. Here c_0 is the (isentropic) sound speed, c_p the specific heat at constant pressure, and γ (= 1.01 for water at 293 K) is the ratio of specific heats . To first and second order (subscript 1 and 2, respectively) we have

$$T = T_0 + T_1 + T_2, \tag{2a}$$

$$p = p_0 + p_1 + p_2, \tag{2b}$$

$$\boldsymbol{v} = \boldsymbol{v}_1 + \boldsymbol{v}_2. \tag{2c}$$

2.1 First-order equations

To first order, the thermodynamic heat transfer equation for T_1, the kinematic continuity equation expressed in terms of p_1, and the dynamic Navier–Stokes equation for the velocity field $\boldsymbol{v}_1$, become

$$\partial_t T_1 = D_\mathrm{th}\nabla^2 T_1 + \frac{\alpha T_0}{\rho_0 c_p}\,\partial_t p_1, \tag{3a}$$

$$\partial_t p_1 = \frac{\rho_0 c_0^2}{\gamma}\Big[\alpha\partial_t T_1 - \boldsymbol{\nabla}\cdot\boldsymbol{v}_1\Big], \tag{3b}$$

$$\rho_0\partial_t\boldsymbol{v}_1 = -\boldsymbol{\nabla}p_1 + \eta\nabla^2\boldsymbol{v}_1 + \beta\eta\,\boldsymbol{\nabla}(\boldsymbol{\nabla}\cdot\boldsymbol{v}_1). \tag{3c}$$

Here (with values for water at room temperature given in parenthesis), D_th is the thermal diffusivity (1.43×10^{-7} m^2/s), α is the volume thermal expansion coefficient (2.07×10^{-4} K^{-1}, c_p is the heat capacity (4.18×10^3 J/(kg K), ρ_0 is the density (997 kg/m^3), η is the dynamic viscosity (10^{-3} Pa s), and β is the viscosity ratio (≈ 0.33). A further simplification can be obtained when assuming all first-order fields to have harmonic time dependence $\exp(-\mathrm{i}\omega t)$, because then p_1 can be eliminated inserting Eq. (3b) with $\partial_t \mathrm{p}_1 = -i\omega p_1$ into Eq. (3a) and (c). Using the thermodynamic identity $T_0\ \alpha^2 c_0{}^2/c_p = \gamma - 1$, we arrive at

$$\mathrm{i}\omega T_1 + \gamma D_\mathrm{th}\nabla^2 T_1 = \frac{1-\gamma}{\alpha}\,\boldsymbol{\nabla}\cdot\boldsymbol{v}_1, \tag{4a}$$

$$\mathrm{i}\omega\boldsymbol{v}_1 + \nu\nabla^2\boldsymbol{v}_1 + \nu\left[\beta + \mathrm{i}\frac{c_0^2}{\gamma\nu\omega}\right]\boldsymbol{\nabla}(\boldsymbol{\nabla}\cdot\boldsymbol{v}_1) = \frac{c_0^2\alpha}{\gamma}\,\boldsymbol{\nabla}T_1. \tag{4b}$$

From Eq. (4) arise the thermal and the viscous penetration depth δ_th and δ, respectively (values for 1 MHz in water),

$$\delta_\mathrm{th} = \sqrt{\frac{2D_\mathrm{th}}{\omega}} \approx 0.2\ \mu\mathrm{m}, \qquad \text{and} \qquad \delta = \sqrt{\frac{2\nu}{\omega}} \approx 0.6\ \mu\mathrm{m}. \tag{5}$$

2.2 Second-order, time-averaged equations

For water, the thermal effects in the above first-order equations are minute because of the smallness of the pre-factor $\gamma - 1 \approx 0.01$. To simplify the following treatment, we therefore neglect the coupling between the mechanical variables $\boldsymbol{v}_2$ and p_2 and the temperature field T_2 in the second-order equations. The second-order continuity equation and Navier–Stokes equation are

$$\partial_t\rho_2 = -\rho_0\boldsymbol{\nabla}\cdot\boldsymbol{v}_2 - \boldsymbol{\nabla}\cdot(\rho_1\boldsymbol{v}_1), \tag{6a}$$

$$\rho_0\partial_t\boldsymbol{v}_2 = -\boldsymbol{\nabla}p_2 - \rho_1\partial_t\boldsymbol{v}_1 - \rho_0(\boldsymbol{v}_1\cdot\boldsymbol{\nabla})\boldsymbol{v}_1 + \eta\nabla^2\boldsymbol{v}_2 + \beta\eta\boldsymbol{\nabla}(\boldsymbol{\nabla}\cdot\boldsymbol{v}_2). \tag{6b}$$

Here, thermal effects enter solely through the temperature-dependent first-order fields ρ_1 and $\boldsymbol{v}_1$. In a typical experiment on acoustic handling of microparticles, the microsecond timescale of the ultrasound oscillations is not resolved. It therefore suffices to treat only the time-averaged equations. The time average of a full oscillation period, denoted by the angled brackets $\langle\cdots\rangle$, of the second-order continuity equation and Navier–Stokes equation becomes

$$\rho_0 \langle \nabla \cdot \boldsymbol{v}_2 \rangle = -\langle \nabla \cdot (\rho_1 \boldsymbol{v}_1) \rangle, \tag{7a}$$

$$\eta \nabla^2 \langle \boldsymbol{v}_2 \rangle + \beta\eta \nabla \Big(\nabla \cdot \langle \boldsymbol{v}_2 \rangle \Big) - \langle \nabla p_2 \rangle = \langle \rho_1 \partial_t \boldsymbol{v}_1 \rangle + \rho_0 \langle (\boldsymbol{v}_1 \cdot \nabla) \boldsymbol{v}_1 \rangle. \tag{7b}$$

It is seen that products of first-order fields act as source terms for the second-order fields. We note that for complex-valued fields $A(t)$ and $B(t)$ with harmonic time-dependence $\exp(-\mathrm{i}\omega t)$, the time average is given by the real-part rule $\langle A(t)\, B(t) \rangle = (1/2)\, \mathrm{Re}[A(0)^*\, B(0)]$, where the asterisk represent complex conjugation.

2.3 Time-averaged acoustic forces on a single suspended particle

Once the first- and second-order acoustic fields have been calculated, it is possible to determine the time-averaged acoustic forces on a single suspended particle. These are the acoustic radiation force $\boldsymbol{F}^{\mathrm{rad}}$ due to the scattering of acoustic waves on the particle and the Stokes drag force $\boldsymbol{F}^{\mathrm{drag}}$ from the acoustic streaming.

It was shown by Settnes and Bruus (2012) that the time-average acoustic radiation force $\boldsymbol{F}^{\mathrm{rad}}$ on a single small spherical particle of radius a, density ρ_{p}, and compressibility κ_{p} is given by

$$\boldsymbol{F}^{\mathrm{rad}} = -\pi a^3 \left[\frac{2\kappa_0}{3} \mathrm{Re}\big[f_1^* p_1^* \nabla p_1 \big] - \rho_0\, \mathrm{Re}\big[f_2^* \boldsymbol{v}_1^* \cdot \nabla \boldsymbol{v}_1 \big] \right], \tag{8}$$

where $\kappa_0 = 1/(\rho_0 c_0{}^2)$ is the compressibility of the fluid, and where the pre-factors f_1 and f_2 are given by

$$f_1(\tilde{\kappa}) = 1 - \tilde{\kappa}, \quad \text{with } \tilde{\kappa} = \frac{\kappa_{\mathrm{p}}}{\kappa_0}, \tag{9a}$$

$$f_2(\tilde{\rho}, \tilde{\delta}) = \frac{2\big[1 - \gamma(\tilde{\delta})\big](\tilde{\rho} - 1)}{2\tilde{\rho} + 1 - 3\gamma(\tilde{\delta})}, \quad \text{with } \tilde{\rho} = \frac{\rho_{\mathrm{p}}}{\rho_0}, \tag{9b}$$

$$\gamma(\tilde{\delta}) = -\frac{3}{2}\Big[1 + \mathrm{i}(1 + \tilde{\delta})\Big]\tilde{\delta}, \quad \text{with } \tilde{\delta} = \frac{\delta}{a}, \tag{9c}$$

The time-averaged Stokes drag force $\boldsymbol{F}^{\mathrm{drag}}$ on a spherical particle of radius a moving with velocity $\boldsymbol{u}$ in fluid having the streaming velocity $\langle \boldsymbol{v}_2 \rangle$ is given by the standard expression

$$\boldsymbol{F}^{\mathrm{drag}} = 6\pi\eta a \big(\langle \boldsymbol{v}_2 \rangle - \boldsymbol{u} \big). \tag{10}$$

3 Numerical model

3.1 Implementation of the governing equations

The governing equations are implemented and solved using the finite element software COMSOL Multiphysics 4.2a. A sequential solution strategy has been used to solve the problem: 1) Solving the first-order acoustic field (given by Eqs. (3a) to (3c)) using the predefined Thermoacoustic Physics Interface in COMSOL. Note that time dependence here is defined as $\exp(\mathrm{i}\omega t)$. 2) The second-order time-averaged flow is then solved by modifying the Creeping Flow Interface, adding a mass source term to the continuity equation and a volume force to the momentum equation. Both terms are calculated from the first-order field. 3) The acoustic radiation forces are directly determined using Eq. (8) and the first-orderfield. 4) Finally, the time-dependent motion of the particles is determined using the COMSOL Particle Tracing Module applying the drag force Eq. (10) and the radiation force to the particles.

When performing the computation spatial care was taken to properly resolve the acoustic boundary layer with an adequate computational mesh. This fine mesh was used when determining the first-order and the second-order time-averaged fields. In the subsequent simulation of the time-dependent motion the flow field and radiation forces where interpolated to a coarser mesh. Using this procedure the transient solving procedure was speeded up substantially.

3.2 Computational domain

We examine a microchannel cross section (width w = 380 µm, height h = 160 µm) as in the microchips developed and used experimentally in the group of Laurell at Lund University [16,18], see Figure 1. In this work we neglect the chip structure, the materials (silicon and pyrex) surrounding the microchannel, as well as the actual piezo actuation of the microchip. Furthermore, we neglect the axial dimension along x, and we only examine the microchannel cross section in the yz-plane. The microchannel is filled with a water suspension of polystyrene particles with diameters of 0.1, 1.0, 3.0 or 5.0 µm. In the model we harmonically actuate the microchannel at 25 ˚C in its half-wave transverse mode by actuation at its resonance frequency of 1.970 MHz, while observing the motion of the polystyrene particles. All model parameters are listed in Table 1 and Section. 2.1.

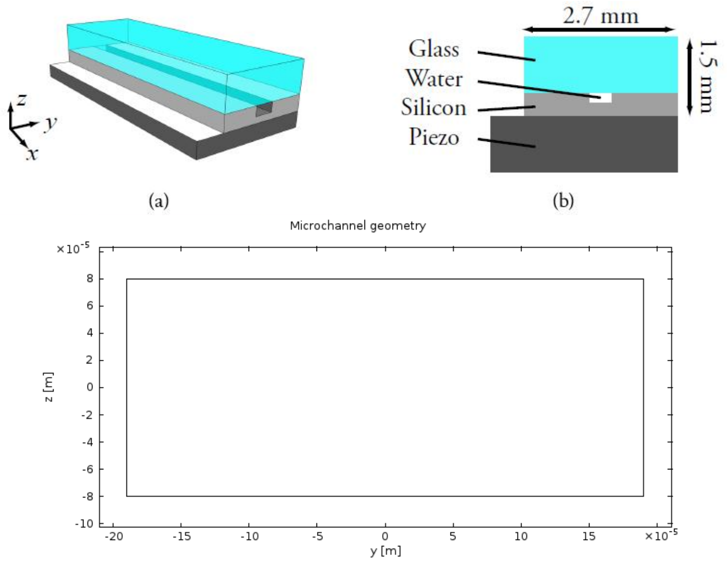

Figure 1: (a-b) Acoustophoresis microchip used in Refs. [16,18]. Figures adapted from Ref. [19]. (c) Microchannel cross section (width w = 380 µm, height h = 160 µm) as modelled in this work. The microchannel is filled with a water suspension of polystyrene particles of 0.1, 1.0, 3.0 or 5.0-µm diameters.

Table 1: Physical parameters used in the model. The parameters are found in the literature at temperature T_0 = 25 ˚C.

Parameter	Symbol	Value
Polystyrene, density	ρ_p	1050 kg m^{-3}
Polystyrene, speed of sound	c_p	2350 m s^{-1}
Polystyrene, Poisson's ratio	σ_p	0.35
Polystyrene, compressibility	κ_p	249 TPa^{-1}
Water, density	ρ_0	997 kg m^{-3}
Water, speed of sound	c_0	1497 m s^{-1}
Water, viscosity	η	0.890 mPa s
Water, compressibility	κ_0	448 TPa^{-1}
Microchannel, height	h	160 µm
Microchannel, width	w	380 µm
Particle diameters	$2a_1$	0.1 µm
	$2a_2$	1.0 µm
	$2a_3$	3.0 µm
	$2a_4$	5.0 µm

4 Results

4.1 First-order pressure and velocity fields

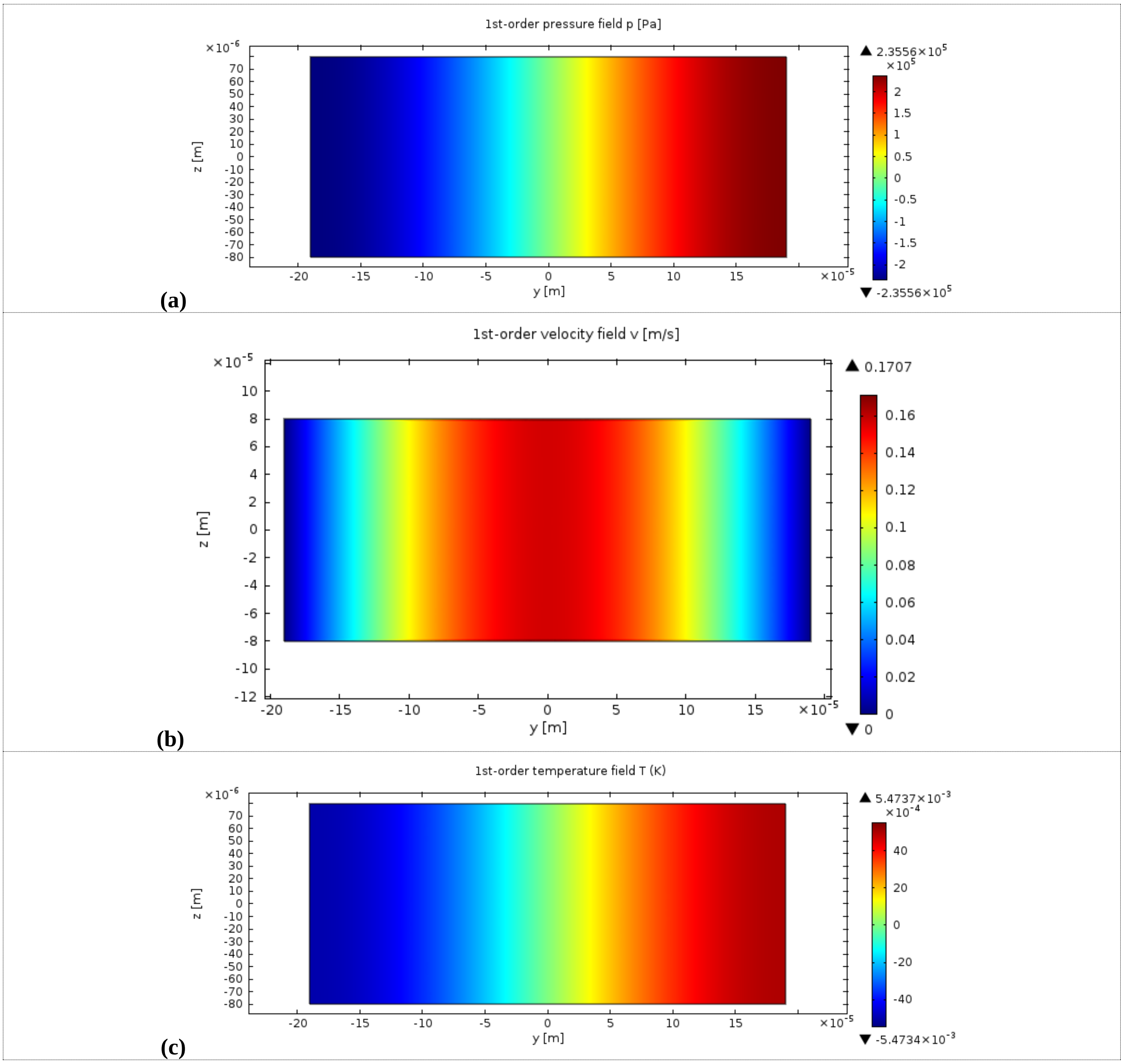

Figure 2: Amplitudes of the harmonic first-order fields; (a) pressure p_1, (b) velocity v_1, and (c) temperature T_1.

4.2 Acoustic streaming velocity field

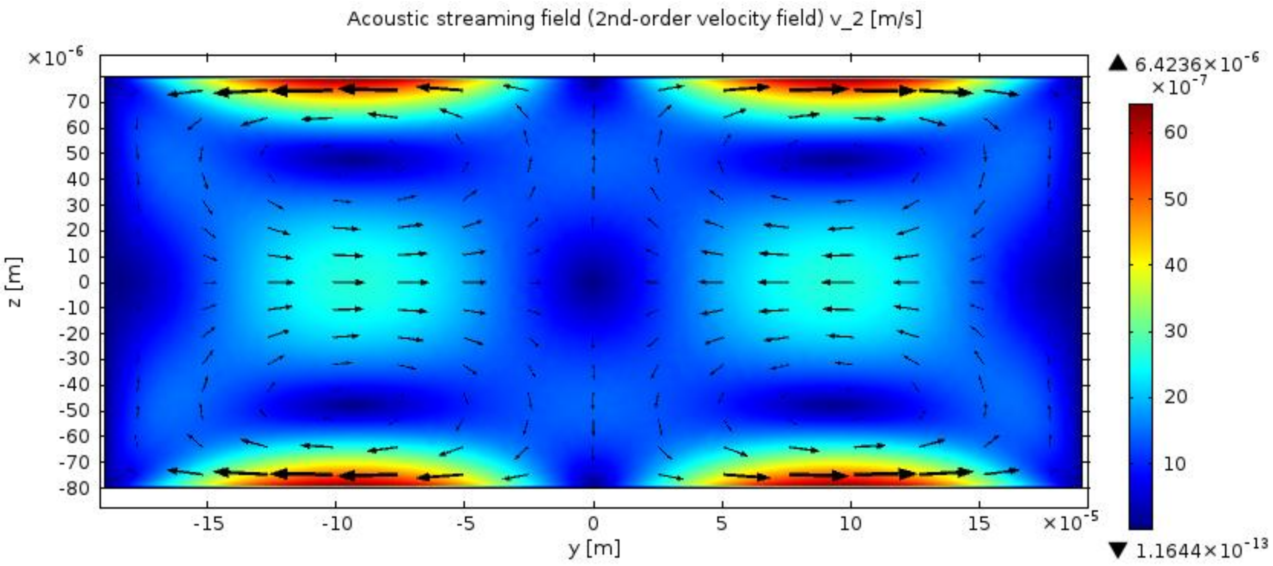

Figure 3: Color and arrow plot of the time-averaged second-order velocity field $\boldsymbol{v}_2$. Four acoustic streaming rolls are generated by the non-linear interactions of the first-order fields.

4.3 Particle trajectories

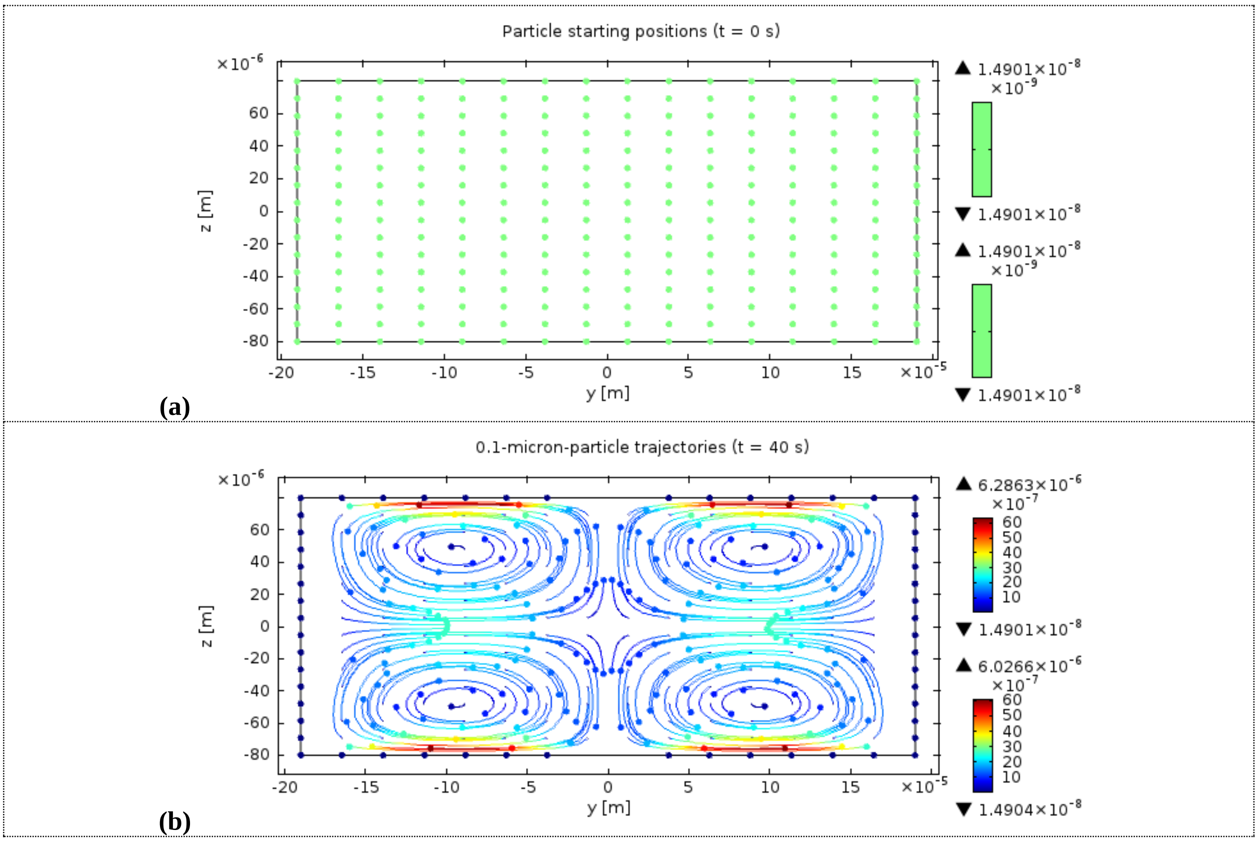

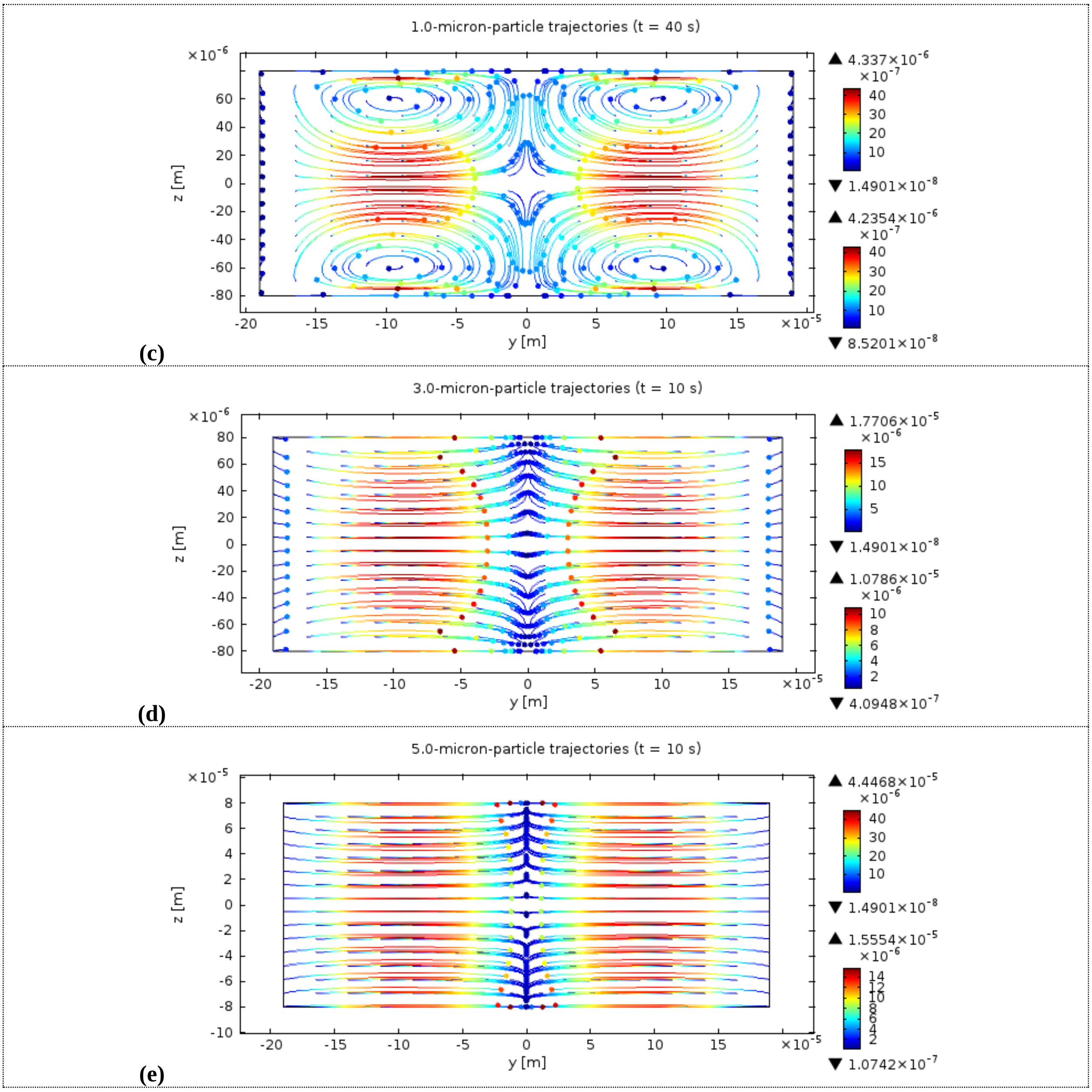

Figure 4: Particle velocities and trajectories. Panel (a) depicts the starting position of the particles. The colour of the particle trajectories indicate the magnitude of the particle velocity. The particle diameters are (b) $2a_1$ = 0.1 µm, (c) $2a_2$ =1 µm, (d) $2a_3$ =3 µm, and (e) $2a_4$ =5 µm. For the small particles the drag force from the acoustic streaming velocity field dominates the particle motion, while for larger particles the acoustic radiation force dominates the particle motion.

5 Conclusions

Using the finite element method the first order acoustic field of a standing wave is determined inside a micro channel cavity by solving the linearized compressional Navier-Stokes equation, the continuity equation, and the entropy equation. The first order field is used to determine the second order time averaged streaming flow and the acoustic radiation forces on micro particles. The time dependent trajectory of the micro particles was finally determined. The different acoustic flow regimes are modelled and related to the particle size.

References

[1] J. Friend and L. Y. Yeo, Rev. Mod. Phys. **83**, 647-704 (2011).

[2] H. Bruus, J. Dual, J. Hawkes, M. Hill, T. Laurell, J. Nilsson, S. Radel, S. Sadhal, and M. Wiklund, , Lab Chip **11**, 3579-3580 (2011).

[3] S. M. Hagsäter, T. G. Jensen, H. Bruus, and J. P. Kutter, Lab Chip **7**, 1336 (2007).

[4] J. Shi, X. Mao, D. Ahmed, A. Colletti, and T. J. Huang, Lab Chip **8**, 221 (2008).

[5] J. Shi, H. Huang, Z. Stratton, Y. Huang, and T. J. Huang, Lab Chip **9**, 3354 (2009).

[6] M. K. Tan, R. Tjeung, H. Ervin, L. Y. Yeo, and J. Friend, Appl. Phys. Lett. **95**, 134101 (2009).

[7] M. K. Tan, L. Y. Yeo, and J. R. Friend, Appl. Phys. Lett. **97**, 234106 (2010).

[8] J. Shi, S. Yazdi, S.-C. S. Lin, X. Ding, I.-K. Chiang, K. Sharp, and T. J. Huang, Lab Chip **11**, 2319 (2011).

[9] O. Manneberg, S.M. Hagsäter, J. Svennebring, H. M. Hertz, J. P. Kutter, H. Bruus, and M. Wiklund, Ultrasonics **49**, 112 (2009).

[10] O. Manneberg, B. Vanherberghen, B. Onfelt, and M. Wiklund, Lab Chip **9**, 833 (2009).

[11] P. Glynne-Jones, R. J. Boltryk, N. R. Harris, A. W. J. Cranny, and M. Hill, Ultrasonics **50**, 68 (2010).

[12] J. D. Adams, P. Thevoz, H. Bruus, and H. T. Soh, Appl. Phys. Lett. **95**, 254103 (2009).

[13] S. Oberti, D. Moeller, A. Neild, J. Dual, F. Beyeler, B. J. Nelson, and S. Gutmann, Ultrasonics **50**, 247 (2010).

[14] C. Ratier and M. Hoyos, Anal Chem **82**, 1318 (2010).

[15] J. D. Adams and H. T. Soh, Appl. Phys. Lett. **97**, 064103 (2010).

[16] R. Barnkob, P. Augustsson, T. Laurell, and H. Bruus, Lab Chip **10**, 563 (2010).

[17] R. Barnkob, I. Iranmanesh, M. Wiklund, and H. Bruus, Lab Chip **accepted**, March (2012).

[18] P. Augustsson, R. Barnkob, S. T. Wereley, H. Bruus, and T. Laurell, Lab Chip **11**, 4152 (2011).

[19] P. Augustsson, PhD Thesis, Lund University, 2 December 2011.

[20] COMSOL Multiphysics 4.2a (www.comsol.com), using the Acoustics Module, the CFD module, and the Particle Tracing Module.